

APPLICATION OF SU8 POLYMER IN WAVEGUIDE INTERFEROMETER AMMONIA SENSOR

M.Bednorz¹, M.Urbańczyk¹, T.Pustelny¹, A.Piotrowska² E.Papis², Z.Sidor², E.Kamińska²

1. *Silesian University of Technology, Institute of Physics, Department of Optoelectronics
ul. Krzywoustego 2, 44-100 Gliwice, Poland*

2. *Institute of Electron Technology, Department of Semiconductor Processing for Photonics Al.
Lotnikow 32/46 02-668 Warsaw, Poland*

The deposition possibility of the polymer based waveguides in low cost and relatively simple and repeatable process is presented in experimental results. The waveguide can be easily formed into Mach-Zehnder interferometer by photolithography. The numerical analysis using the beam propagation method yields very promising results of sensor interaction with ammonia. The aim of future work will be to deposit the desired interferometer and compare the efficiency of the sensor with computer analysis.

1. INTRODUCTION

Recent growth of organic materials technology including polymers provides the new materials for waveguide layers in integrated optics circuits. One of the most frequently investigated and employed materials is the SU8 photoresist based on an epoxy monomer SU8. Because of mechanical properties, thermal and chemical stability and ease of fabrication of desired designs this UV-negative-tone photoresist is being applied in many MEMS and MOEMS devices. The most important features as far as the optoelectronics is concerned are high transparency in visible and near IR region of spectrum and refractive index about 1.5 in visible region of spectrum. This allows producing the desired low loss strip waveguides circuit employing the standard photolithography process [1-3]. Also the waveguides sensors based on SU8 waveguides has been reported. The authors of [4] present the SU8 strip waveguides Mach-Zehnder interferometer designed as immunosensor.

2. WAVEGUIDE FABRICATION

The first attends of employing the SU8 technology has been made in the Institute of Electron Technology in Warsaw. The photoresist under consideration was the GM10-40 type purchased at Gersteltec. In order to optimize the process parameters many samples have been

deposited and their thickness has been measured by TENCOR alpha-step 200 profiler. The waveguides have been deposited at the glass substrate in standard photolithography process including spin coating by using Brewer 100CB hotplate/spinner and UV exposure (K. Süss MJB 3 UV250/300/400 aligner) forming 4 μm and 6 μm wide stripes. Depending on rotation speed different thickness of layers has been deposited (Fig. 1).

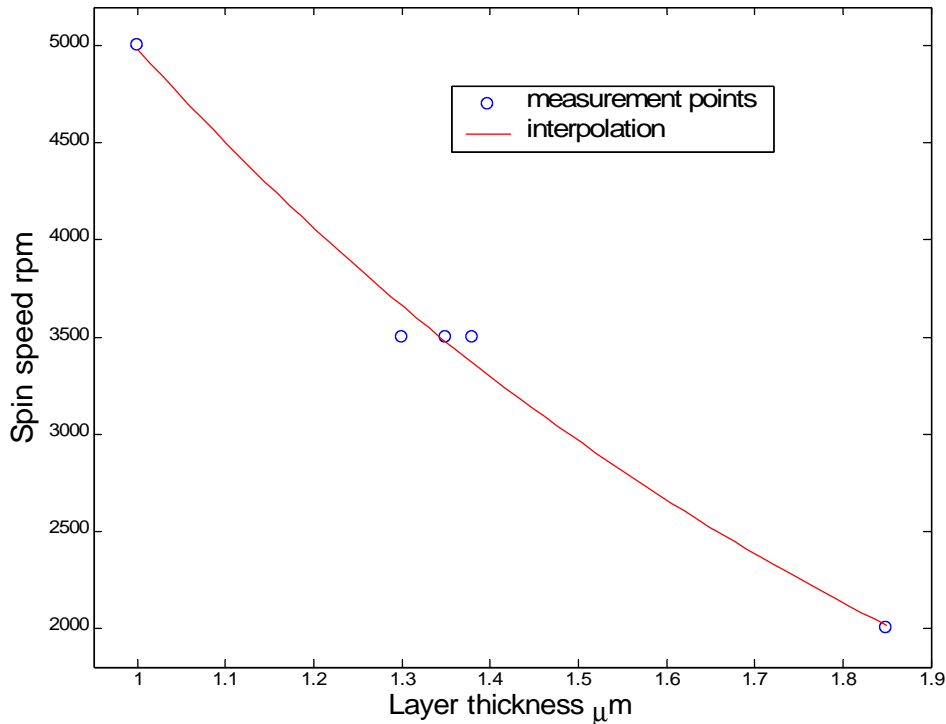


Fig. 1. Deposited layer thickness versus spin speed

Insignificant discrepancy of the achieved thickness for 3500 rpm arises probably from the insufficient temperature control during the whole process. The microscope pictures of deposited stripes have been presented below, in Fig. 2:

These studies have shown the possibility of deposition the predefined waveguides and waveguide circuit in low cost and relatively simple and repeatable process.

Unfortunately the attempts of introducing the light into fabricated stripe waveguides have not been made. One of the ways of introducing the light into stripe waveguides is face coupling, which demands smooth edge that can be easily achieved for silicon wafer by cleaving. In case of glass substrate the task is much more complicated. The further research will employ the silicon wafers with oxidized surface as substrates.

The refractive index of fabricated SU8 layers has been measured in Institute of Electron Technology with J.A.Woollam Variable Angle Spectral Ellipsometer (VASE) in the spectral range 240-1100 nm. The refractive index wavelength dependency has been shown at Fig. 3.

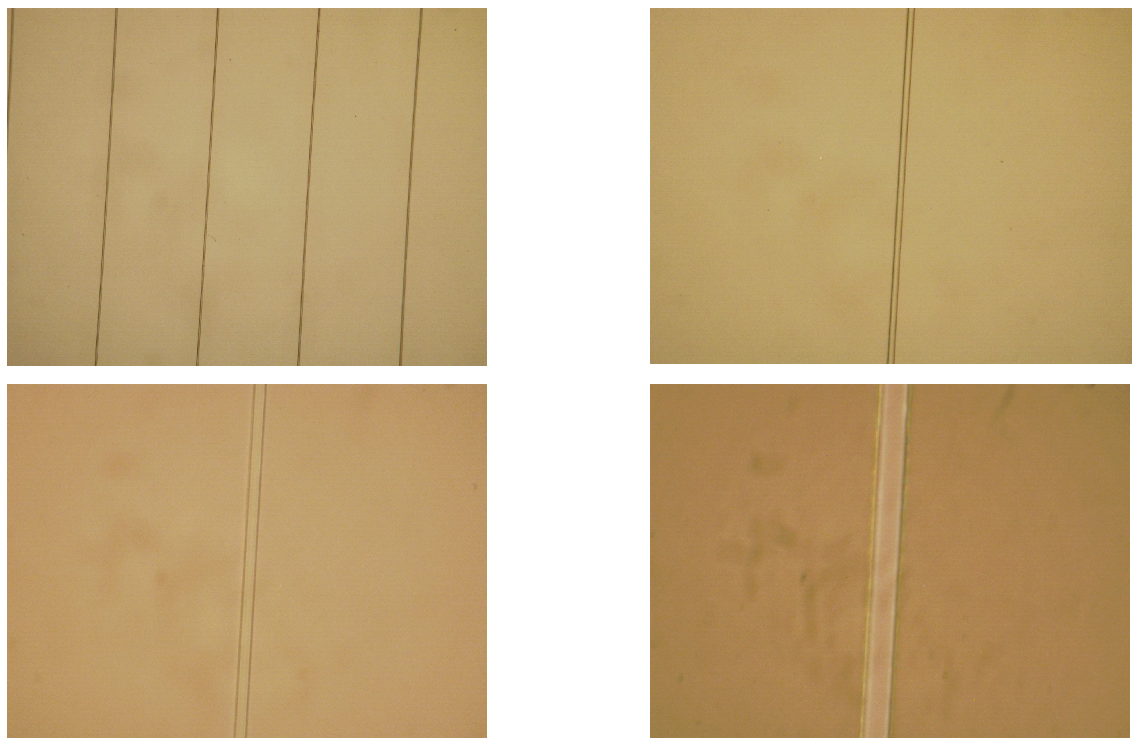


Fig. 2. Microscope picture of deposited SU8 polymer stripes of width ranging from 6.4 to 6.7 μm (precision of measurement 0.1 μm).

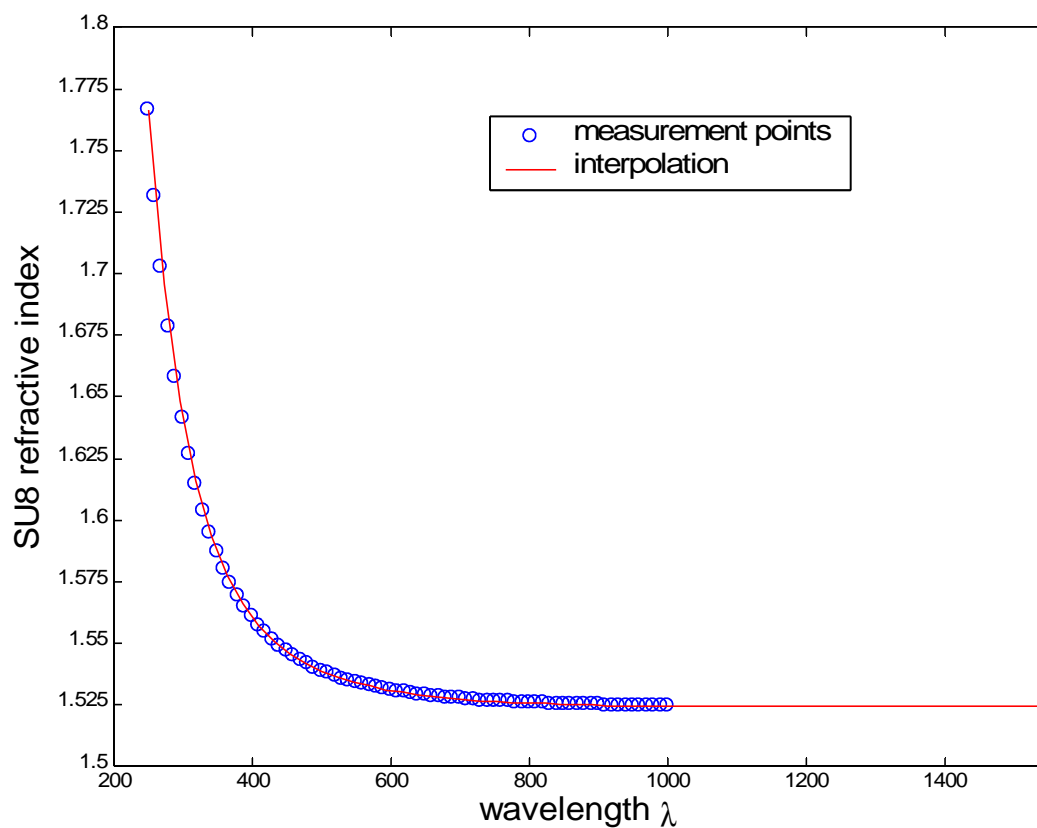


Fig. 3. SU8 refractive index dispersion, measured with VASE ellipsometer at ITE

The authors of [4] report that the value of SU8 refractive index can be altered by high temperature post-process annealing. The 3 minutes long heating at 200°C resulted in decrease of n by 0.004. This method can be employed to fabricate waveguides from SU8 with uncured core and cured low index cladding [4].

3. PROPOSED SENSOR STRUCTURE

Proposed sensor structure is based on Mach-Zehnder interferometer made of SU8 photolithography deposited stripe waveguides (Fig. 4).

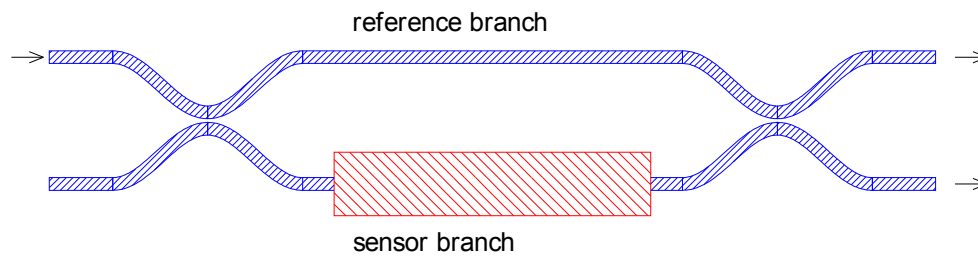


Fig. 4. Sensor structure scheme – waveguide Mach-Zehnder interferometer.

The substrate is silicon wafer with oxidized surface. The waveguides are buried in second SiO_2 layer.

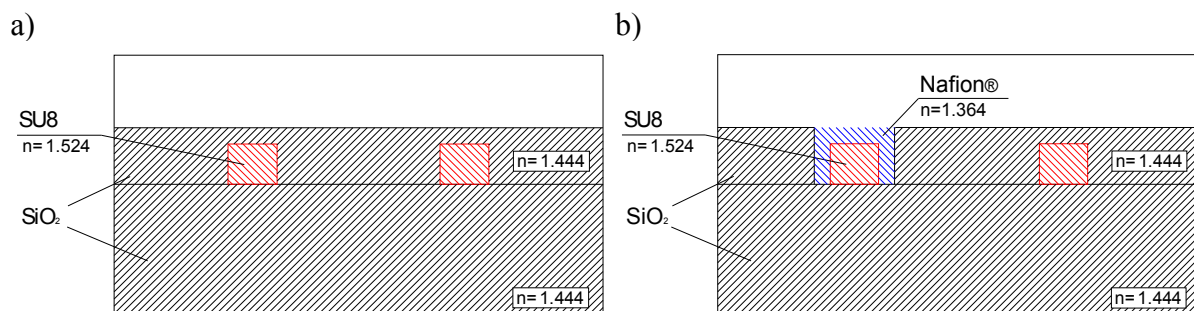


Fig. 5. Cross-section of sensor structure, a) input area, b) sensing window area

4. BPM ANALYSIS OF PROPOSED STRUCTURE

In order to simulate the operation of sensor and to optimize the shape, dimensions and used materials of sensor structure the numerical analysis with beam propagation method has been proposed.

The analysis has been carried with Optiwave software – OptiBPM. The first task was to determine the optimal geometrical shape, dimensions and appropriate materials providing the single mode propagation. The BPM method is based on paraxial approximation hence it is unusable for the waveguide structures with considerable difference of refractive index between layers in transverse plane. For the sake of these limitations the SU8 waveguides with air cladding have not been considered. Two different claddings has been investigated SiO_2 and

MgF₂, the refractive index at wavelength 1.55 μm is respectively 1.444 and 1.3809. These layers can be deposited at the top of SU8 waveguides by magnetron sputtering.

The determination of single mode conditions has been performed with OptiBPM ModeSolver. The required dimensions are the same for two examined claddings:

- waveguide thickness – 1.3 μm
- waveguide width – 2 μm

The table 1 summarizes the determined effective indexes of guided modes depending on solver, analyzed field and boundary conditions.

Table 1 Effective indexes of guided modes

Solver	Mode	Boundary conditions	Cladding	Effective index of guided mode
Real	Semi-Vector TE	Dirichlet	SiO ₂	1,46999466
Real	Semi-Vector TE	Neuman	SiO ₂	1,46999684
Real	Full Vector Along x	Dirichlet	SiO ₂	1,46999625
Real	Semi-Vector TE	Dirichlet	MgF ₂	1,46130532
Real	Semi-Vector TE	Neuman	MgF ₂	1,46131467
Complex	Full Vector Along x	TBC	MgF ₂	1,46120523

The important part of beam propagation analysis was the determination of optimal computational mesh step and BPM propagation step in z direction. The finer mesh and propagation step improve the fidelity and accuracy of results, but can strongly hamper the speed of calculation.

The waveguide under inspection was a section of bend arc waveguide and X coupler (Fig. 6).

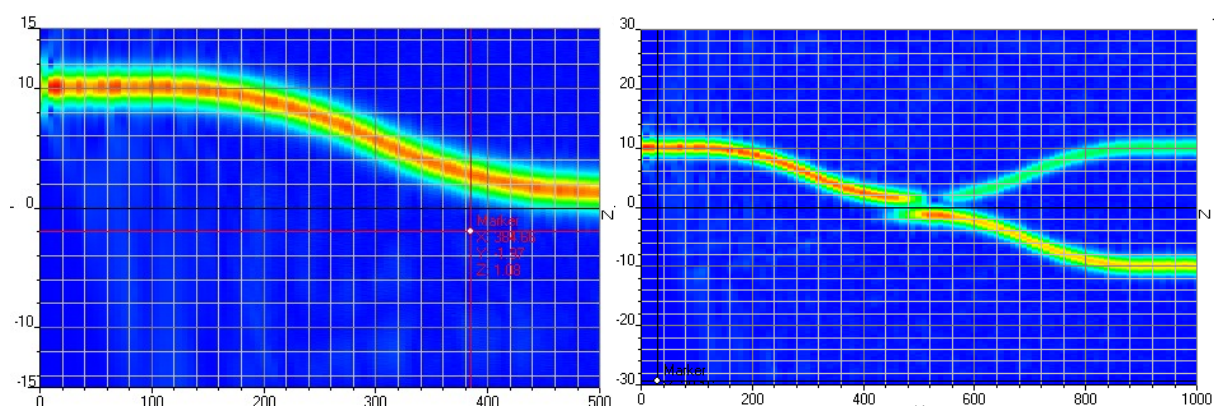


Fig. 6. Optical field in investigated waveguides

The sizes of computational window are:

1. x-width – arc – 30 μm , X coupler – 60 μm
2. y-thickness - 8 μm
3. z-length – arc – 500 μm , X coupler – 1000 μm

The results for different propagation steps have been depicted below:

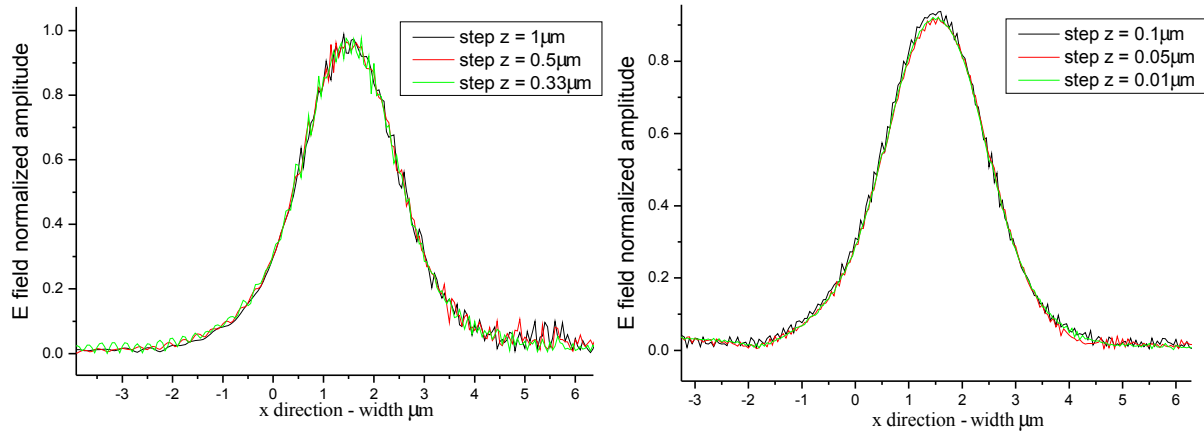


Fig 7 E field amplitude at the end of arc waveguide for different propagation steps

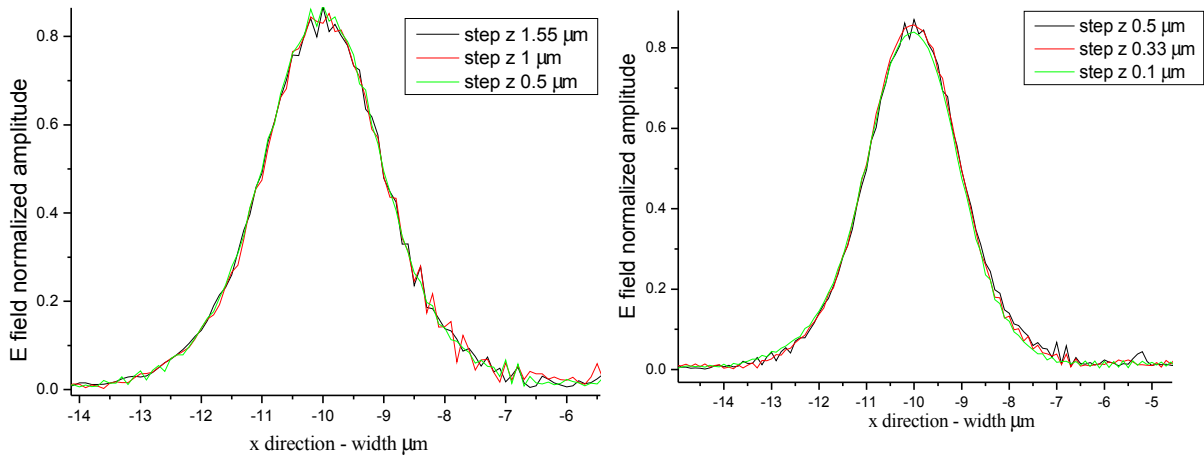


Fig. 8. E field amplitude in one of output branches of X coupler for different Δz .

Presented results show that finer z-step improves the accuracy and eliminate the noise caused by huge leaps in algorithm over the regions of bend where the refractive index in transverse plane changes rapidly with every propagation step. Hence the slowly varying envelope approximation is no longer valid in these regions. The value of optimal step Δz seems to be $0.1\mu\text{m}$ and this value was default in further investigations.

5. SIMULATION OF SENSOR OPERATION - RESULTS

In order to simulate the sensor operation the BPM analysis of SU8 buried waveguide Mach-Zehnder interferometer has been performed. One of the interferometer branches is covered with sensor layer Nafion® which refractive index or thickness is being altered simulating the interaction with gas.

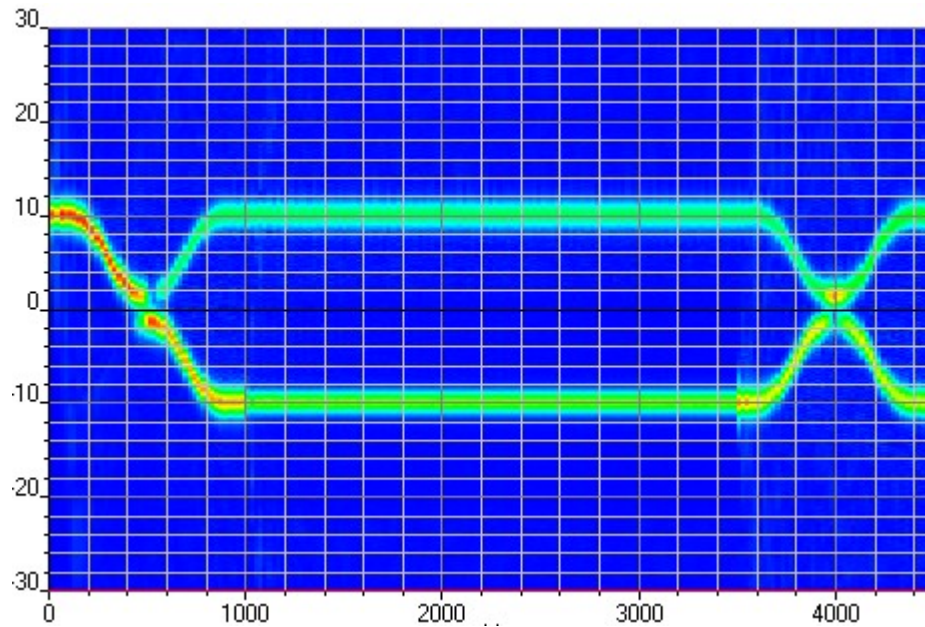


Fig 9 Optical field in Mach-Zehnder interferometer.

The sensor response has been acquired from power distribution between to output waveguides of X output coupler, changing in every iteration of program loop in which the refractive index is increased by 0.001 corresponding to interaction with 50ppm of ammonia [5]. The analysis has been performed with different mesh size and propagation steps in order to determine the influence of these parameters on sensor efficiency.

The conclusion arising from results presented on following pages proves that variation of sensor layer refractive index due to interaction with gas changes the coupling efficiency for two output arms of out X coupler. The choice of mesh parameters and propagation steps also impacts the results and sensitivity, but on the grounds of previous investigations we can assume that results achieved with $0.1\mu\text{m}$ propagation step reflect the reality. The transverse mesh step size has also been optimized in case of Δy the value $0.0066\mu\text{m}$ (150 nodes/ $1\mu\text{m}$) arise from the fact the analysis with changing of sensor layer thickness by $0.01\mu\text{m}$ has been and will be conducted. So the Δy mesh step must be finer than $0.01\mu\text{m}$ in all cases to produce comparable results. As can be seen from comparison of Fig. 11 and Fig. 13 the MgF_2 cladding is slightly more sensitive in region of Nafion® refractive index. The power in output waveguides changes by 0.3 whereas in case of SiO_2 it is less than 0.2.

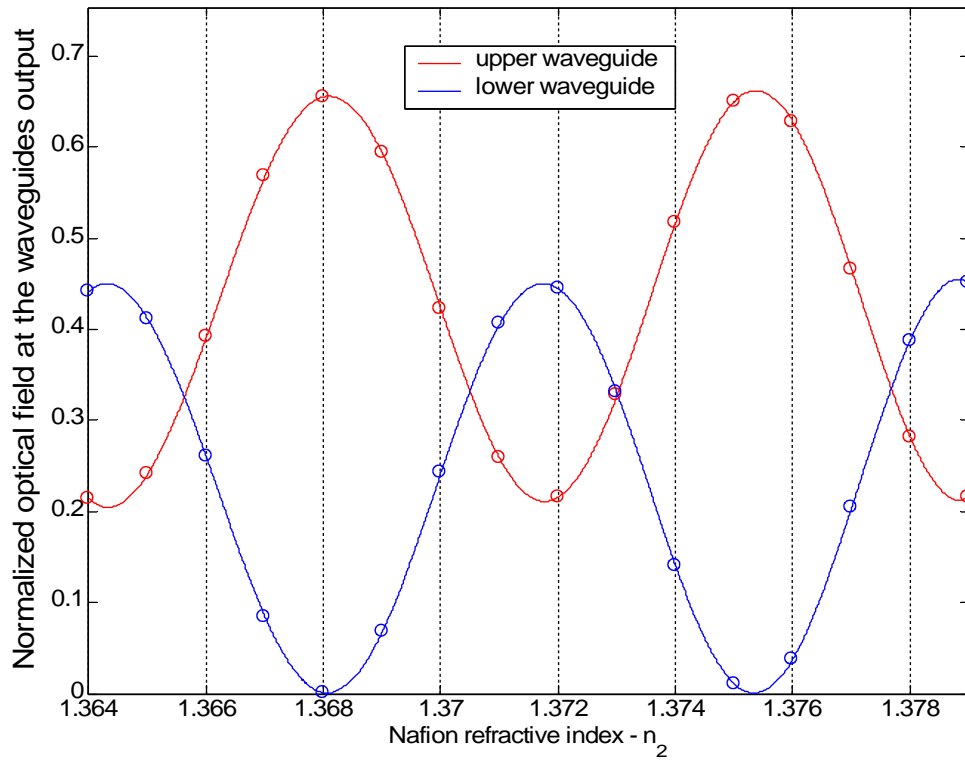


Fig. 10. Simulation of sensor response due to changes of sensor layer refractive index, cladding layer SiO₂, mesh parameters – Δx step 0.1 μm , Δy step 0.01 μm , Δz step 1.55 μm .

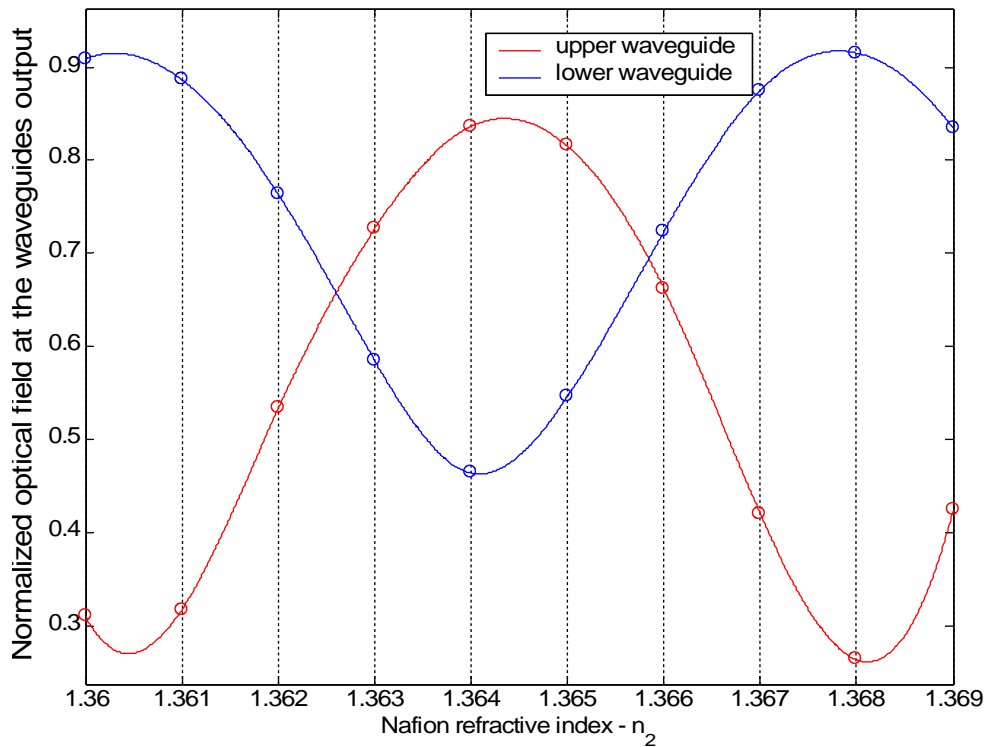


Fig. 11. Simulation of sensor response due to changes of sensor layer refractive index, cladding layer SiO₂, mesh parameters – Δx step 0.025 μm , Δy step 0.0067 μm , Δz step 0.1 μm .

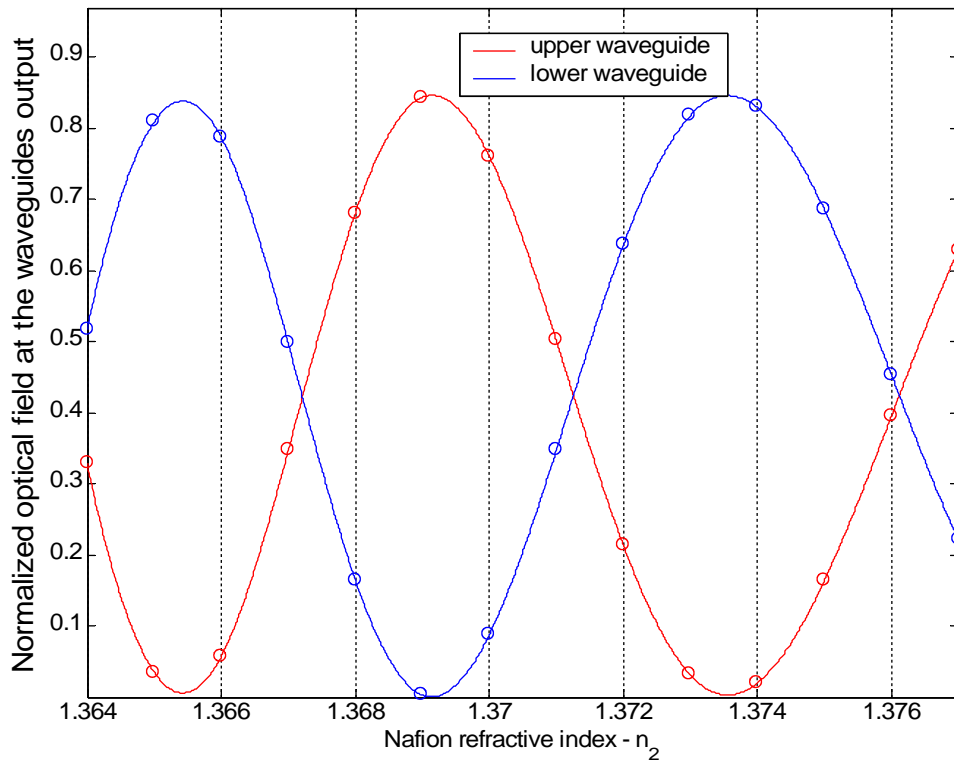


Fig. 12. Simulation of sensor response due to changes of sensor layer refractive index, cladding layer MgF_2 , mesh parameters – Δx step $0.1\mu\text{m}$, Δy step $0.01\mu\text{m}$, Δz step $1.55\mu\text{m}$.

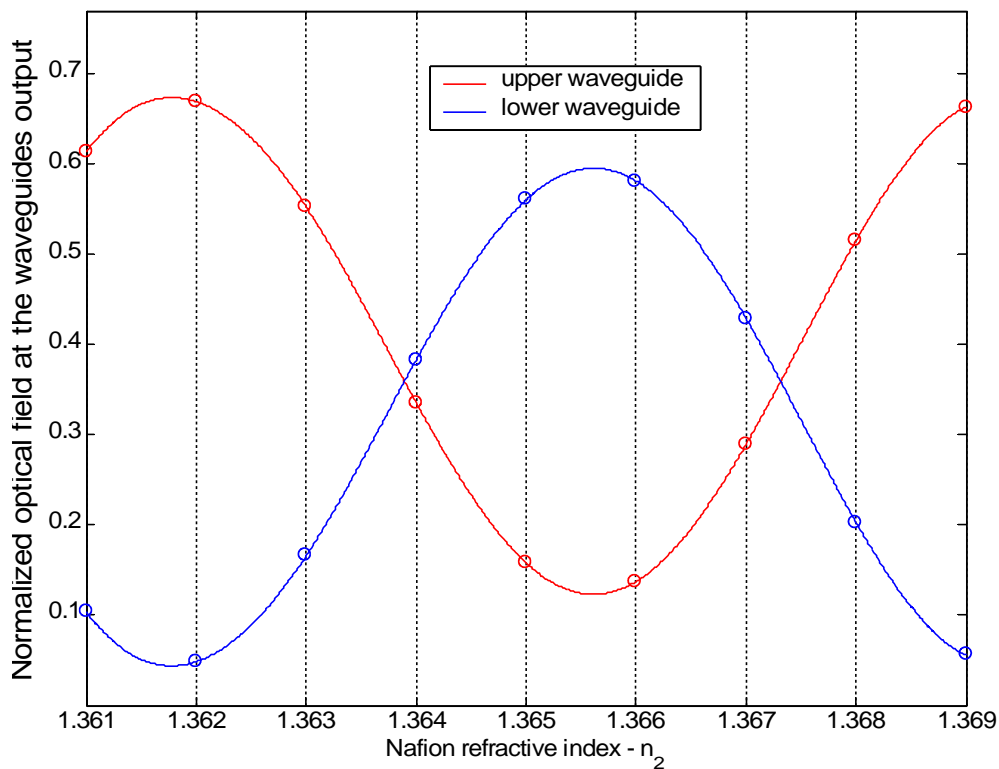


Fig. 13. Simulation of sensor response due to changes of sensor layer refractive index, cladding layer MgF_2 , mesh parameters – Δx step $0.025\mu\text{m}$, Δy step $0.0067\mu\text{m}$, Δz step $0.1\mu\text{m}$.

6. CONCLUSION

Presented experiment results show the possibility of deposition the polymer based waveguides in low cost and relatively simple and repeatable process. The waveguide can be easily formed into Mach-Zehnder interferometer by photolithography. The numerical analysis using the beam propagation method yields very promising results of sensor interaction with ammonia. The aim of future work will be to deposit the desired interferometer and compare the efficiency of the sensor with computer analysis.

REFERENCES

1. B. Beche, N. Pelletier, E. Gaviot, J. Zyss, Single-mode TE₀₀–TM₀₀ optical waveguides on SU-8 polymer, *Optics Communications*, 230, 91–94, (2004).
2. Polymeric optical waveguides using direct ultraviolet photolithography process, *Applied Physics A*, 80, Issue: 3, February 2005, pp. 621 - 626 Tung, K.K.; Wong, W.H.; Pun, E.Y.B.
3. Ansel Y. et al, Optical waveguide device realised using two SU8 layers, *Proc Optical MEMS* (2002)
4. B.Y. Shewa, C.H. Kuo, Y.C. Huang, Y.H. Tsai, UV-LIGA interferometer biosensor based on the SU-8 optical waveguide, *Optics Communications*, 230, 91–94, (2004).
5. M. Bednorz, A. Stolarczyk, E. Maciak, T. Pustelny, Z. Opilski, M. Urbańczyk, Influence of humidity variations on performance of Nafion® based ammonia optical sensor, *Journal de Physique IV*, 137, 23-29, (2006).